Geophysical Research Letters

RESEARCH LETTER
10.1029/2021GL096602

An Atmospheric Bridge Between the Subpolar and Tropical Atlantic Regions: A Perplexing Asymmetric Teleconnection

Seung H. Baek[1], Yochanan Kushnir[2], Walter A. Robinson[3], Juan M. Lora[1], Dong Eun Lee[4], and Mingfang Ting[2]

[1]Department of Earth and Planetary Sciences, Yale University, New Haven, CT, USA, [2]Lamont-Doherty Earth Observatory, Columbia University, Palisades, NY, USA, [3]Department of Marine, Earth, and Atmospheric Sciences, North Carolina State University, Raleigh, NC, USA, [4]Department of Marine Environmental Sciences, ChungNam National University, Daejeon, South Korea

Key Points:

- A fast, basin-wide atmospheric response to Atlantic subpolar gyre sea surface temperature (SST) anomalies connects the subpolar and tropical Atlantic regions
- This "atmospheric bridge" communicates, via wind-driven evaporative cooling, only cold subpolar Atlantic SSTs to the tropical Atlantic
- The atmospheric bridge does not effectively communicate warm subpolar Atlantic SSTs, highlighting an important asymmetry of AMV

Supporting Information:

Supporting Information may be found in the online version of this article.

Correspondence to:

S. H. Baek,
seunghun.baek@yale.edu

Citation:

Baek, S. H., Kushnir, Y., Robinson, W. A., Lora, J. M., Lee, D. E., & Ting, M. (2021). An Atmospheric bridge between the subpolar and tropical Atlantic regions: A perplexing asymmetric teleconnection. *Geophysical Research Letters*, *48*, e2021GL096602. https://doi.org/10.1029/2021GL096602

Received 13 OCT 2021
Accepted 8 DEC 2021

Abstract The largest sea surface temperature (SST) anomalies associated with Atlantic Multidecadal Variability (AMV) occur over the Atlantic subpolar gyre, yet it is the tropical Atlantic from where the global impacts of AMV originate. Processes that communicate SST change from the subpolar Atlantic gyre to the tropical North Atlantic thus comprise a crucial mechanism of AMV. Here we use idealized model experiments to show that such communication is accomplished by an "atmospheric bridge." Our results demonstrate an unexpected asymmetry: the atmosphere is effective in communicating cold subpolar SSTs to the north tropical Atlantic, via an immediate extratropical atmospheric circulation change that invokes slower wind-driven evaporative cooling along the Eastern Atlantic Basin and into the tropics. Warm subpolar SST anomalies do not elicit a robust tropical Atlantic response. Our results highlight a key dynamical feature of AMV for which warm and cold phases are not opposites.

Plain Language Summary To investigators of Atlantic Multidecadal Variability (AMV), one outstanding conundrum is the discrepancy between where the largest AMV changes occur (subpolar North Atlantic) and where the remote impacts of AMV originate (tropical North Atlantic). Processes that communicate sea surface temperature (SST) changes from the subpolar gyre region to the tropical North Atlantic are a potentially crucial but poorly understood aspect of AMV. Here, using idealized model experiments, we investigate the idea that such communication is accomplished by an "atmospheric bridge"—a fast, basin-wide atmospheric response to subpolar gyre SST anomalies that produces a tropical SST change. Our results demonstrate an unexpected, but robust asymmetry: The atmosphere is effective in communicating, via a fast circulation change that invokes wind-driven evaporative cooling along the Eastern Basin, only *cold* SST anomalies from the Atlantic subpolar gyre to the tropical North Atlantic. In contrast, imposed warm subpolar SST anomalies do not elicit a tropical Atlantic response. Our results highlight a key dynamical feature of AMV for which warm and cold phases are not opposites.

1. Introduction

The Atlantic Multidecadal Variability (AMV) is characterized by warming and cooling of North Atlantic sea surface temperature (SSTs) in a coherent, horseshoe pattern (Delworth & Mann, 2000; Enfield et al., 2001; Kushnir, 1994; Schlesinger & Ramankutty, 1994). AMV is dynamically linked to changes in the North Atlantic Subtropical High (Hu et al., 2011; Kushnir et al., 2010) and is purported to drive extensive global climate anomalies (Knight et al., 2006; Zhang & Delworth, 2006). States of the AMV are associated with hydroclimate variability over North America (Hu et al., 2011; Kushnir et al., 2010; Sutton & Hodson, 2007), the Euro-Mediterranean region (Kushnir & Stein, 2010; Zampieri et al., 2017), and northeast Brazil (Hastenrath & Greischar, 1993; Knight et al., 2006), as well as alternating wet/dry conditions over India (Naidu et al., 2020; Zhang & Delworth, 2006) and the Sahel (Folland et al., 1986; Knight et al., 2006; Kushnir & Stein, 2010; Zhang & Delworth, 2006).

Despite its extensive impacts, many dynamical features of AMV remain poorly understood (Bellomo et al., 2018; Booth et al., 2012; Brown et al., 2016; Buckley et al., 2015, 2014; Clement et al., 2015; Murphy et al., 2017; Otterå et al., 2010; Terray, 2012; Ting et al., 2009; Zhang et al., 2013; 2019). One such issue is the discrepancy between where the largest AMV SST changes occur (Ting et al., 2009) and where the remote impacts of AMV are forced (Ruprich-Robert et al., 2017). The largest AMV SST changes, as well as distinctly decadal and longer

SST variability, occur in the Atlantic subpolar gyre where there is a strong role for the circulation of the ocean and its large thermal capacity (Knight et al., 2005, 2006; Sutton et al., 2018; Terray, 2012; Ting et al., 2009). Yet, it is the tropical lobe of the AMV SST pattern that is primarily responsible for forcing the remote impacts of AMV (Chiang et al., 2008; Kushnir et al., 2010; Ruprich-Robert et al., 2017; Zhang et al., 2019).

That the Atlantic subpolar gyre is the region of greatest AMV SST change is consistent with an understanding of AMV as the consequence of multidecadal variations in the Atlantic Meridional Overturning Circulation (AMOC). It has been postulated that strong overturning enhances North Atlantic heat transport to the subpolar Atlantic gyre, which results in warm phases of the AMV and vice versa (Buckley & Marshall, 2016; Delworth & Mann, 2000; Knight et al., 2005; Oelsmann et al., 2020; Zhang et al., 2019). Although not directly confirmed by observations (Lozier, 2010), indirect proxies of oceanic circulation suggest AMOC leads AMV (Sutton et al., 2018; Zhang et al., 2019). This theory, however, is still debated. Clement et al. (2015) in particular showed that climate models coupled to a motionless mixed-layer representation of the ocean, with prescribed heat flux correction that emulates "climatological" ocean heat transport, can simulate the AMV spatial pattern of variability in the North Atlantic (including concentrated SST loading on the subpolar Atlantic), suggesting that the phenomenon could be the response of the ocean mixed layer to local surface heat flux exchanges with the atmosphere. A role for external radiative forcing from changes in greenhouse gas and aerosol concentrations (Bellomo et al., 2018; Booth et al., 2012; Murphy et al., 2017; Otterå et al., 2010) has also been proposed.

Regardless of the source of AMV, anomalies in atmospheric circulation are expected to play a vital role in communicating its SST anomalies from the Atlantic subpolar gyre to the tropical North Atlantic (Martin et al., 2014; Yuan et al., 2016). Such atmospheric processes comprise a crucial component of how the remote impacts of the AMV are propagated, but they remain poorly characterized. Here we aim to improve our mechanistic understanding of such a subpolar-to-tropics "atmospheric bridge" using atmospheric model ensembles coupled to a slab ocean. We impose warming and cooling over the subpolar Atlantic that forces SST anomalies resembling those of warm and cold phases of the AMV. The slab ocean experiments are supplemented with counterpart experiments that employ a 3-dimensional, fully dynamical ocean with similarly imposed subpolar AMV anomalies. Notably, atmospheric responses in these idealized model experiments display an unexpected asymmetry: The atmosphere effectively bridges only *cold* SST anomalies from the Atlantic subpolar gyre to the tropical North Atlantic.

2. Methods

2.1. Parsing Internal and Forced Components of the AMV

Current understanding of observed AMV views the phenomenon as consisting of an internal component inherent to the coupled climate system and an external component driven by historical radiative forcings. We follow Ting et al. (2009) in applying a signal-to-noise maximizing empirical orthogonal functions (EOF) analysis to observed global SSTs. This separates internally generated positive and negative phases of the AMV from the radiatively forced 20th century SST change (see Ting et al., 2009 for details). We use the subpolar North Atlantic section of the pattern attributed to positive and negative phases of internal variability for our subsequent model experiments.

2.2. Slab Ocean Model Experiments

We employe three 60-member ensembles of the Community Atmospheric Model version 5.0 (CAM5; Hurrell et al., 2013). The atmospheric model is coupled to an interactive slab ocean over the Atlantic from 30°S to 90°N, with SST prescribed to vary according to the observed 1970–2000 climatological annual cycle everywhere else in the world ocean. The Atlantic slab temperature is surface heat flux-corrected (Q-flux) to maintain, on average, the observed monthly SST climatology during 1970–2000. Over the subpolar North Atlantic (north of 45°N), the Q-flux-corrected SSTs in each respective ensemble are relaxed to three different states. In the first ensemble, the subpolar North Atlantic is maintained at its observed climatology over 1970–2000 (denoted CLM-ML for climatological-mixed layer). In the second ensemble, the subpolar North Atlantic is maintained at the observed SST climatology plus five times the positive AMV pattern north of 45°N (POS-ML for positive-mixed layer); in the third ensemble, the subpolar area is maintained at the observed SST climatology minus five times the negative AMV pattern north of 45°N (herein NEG-ML for negative-mixed layer). Assuming linearity, amplifying the subpolar AMV patterns beyond the positive or negative AMV patterns generates a more robust response (see Lee et al., 2018). All observed SSTs are from the Hadley Centre Sea Ice and Sea Surface Temperature dataset

version 1 (HadISSTv1). For sea ice, the Community Ice CodE version 4 (CICE4; Hunke & Lipscomb, 2008) is coupled to CAM5. The CICE4 model calculates surface fluxes, albedo, snow depth, and surface temperature over the ice area, while sea ice concentration is prescribed to 1970–2000 climatological values and sea ice thickness is maintained at 2 meters for the Arctic and 1 meter for the Antarctic. All experiments are run 60 times, each for 13 months starting on August 31st. The initial atmospheric conditions for each ensemble member are randomly picked from a continuous control simulation forced with observed climatological SSTs. Outputs from the slab-ocean model experiments have ∼2.8 grid resolution.

2.3. Fully-Coupled Model Experiments

We also analyze the output of two 30-member ensembles of the fully coupled Community Earth System Model version 1.0 (CESM1; Hurrell et al., 2013) run to study the global climate response to the AMV (see Castruccio et al., 2019; Ruprich-Robert et al., 2017). These ensembles are analogous in design to POS-ML and NEG-ML, but the atmospheric model is coupled to a 3-dimensional, dynamical ocean (denoted SPG_AMV+ and SPG_AMV−, respectively). Model SSTs are allowed to evolve freely except in the subpolar North Atlantic (37° to 73°N), where SST anomalies corresponding to plus (SPG_AMV+) or minus (SPG_AMV−) one standard deviation of the observed AMV index are imposed in accordance with Ting et al. (2009). Two 8° latitude buffer zones are imposed at the northern and southern boundaries of the subpolar North Atlantic, where the restoring coefficient is decreased by 0.125 per degree of latitude; full restoring is thus only applied between 45° and 65°N. Outputs from the fully-coupled model experiments have 0.94° latitude by 1.25° longitude grid resolution.

To approximate control runs (CLM*; see below for details), we employ two additional 30-member ensembles of the fully coupled CESM1 model that allow model SSTs to evolve freely except over the entire North Atlantic (0°N to 73°N), where SST anomalies corresponding to plus or minus one standard deviation of the observed AMV index are imposed in accordance with Ting et al. (2009; herein Full_AMV+ and Full_AMV−, respectively). Here too 8° latitude buffer zones are imposed at the northern and southern boundaries of the North Atlantic, where the restoring coefficient is decreased by 0.125 per degree of latitude; full restoring is thus only applied between 8°N and 65°N. All fully coupled experiments are run continuously for 10 years, starting in January. See Ruprich-Robert et al. (2017) and Castruccio et al. (2019) for additional details on the experimental setups of SPG_AMV+, SPG_AMV−, Full_AMV+, and Full_AMV−.

2.4. Model Analysis

Members of a given model ensemble have a forced component (climatological component for control runs) over the subpolar Atlantic that is common across the ensemble, but the members vary in their realizations of internal variability. For the slab-ocean model runs, internal variability comes from the atmosphere and its surface heat exchange with the Atlantic Ocean mixed-layer, as SSTs over the rest of the ocean are prescribed. For fully coupled experiments, internal variability comes from the atmosphere and its interaction with the global ocean. Averaging across a large ensemble reduces internal variability, such that the ensemble mean can be interpreted as the forced response (climatological response for control runs) to a given experiment. Subtracting the ensemble mean of CLM-ML from the ensemble means of NEG-ML and POS-ML, respectively, thus isolates the influence of the subpolar AMV forcing in the atmospheric model experiments.

For the CESM1 fully coupled model experiments, we approximate the climatological component of surface temperature (and the only surface temperature) in the CESM1 fully coupled experiments (herein CLM*) by taking the average of Full_AMV+ and Full_AMV−. We then subtract CLM* from ensemble means of SPG_AMV− and SPG_AMV+ to isolate the influences of subpolar forcing on the temperatures. We do not use the average of SPG_AMV+ and SPG_AMV− to approximate CLM* because of suspected asymmetric responses in the tropical Atlantic driven by warm and cool subpolar North Atlantic forcings in SPG_AMV+ and SPG_AMV−; such asymmetric responses are limited in Full_AMV+ and Full_AMV− because observed AMV SST anomalies are imposed on *both* the tropical North Atlantic and subpolar North Atlantic. Adding together Full AMV+ and Full AMV− thus roughly reduces the AMV amplitude over the North Atlantic region to zero. Our approximation of CLM* only applies to surface temperature because no observed AMV anomalies are imposed for other climate variables. We furthermore note that our CLM* approximation method may not be applicable outside the North

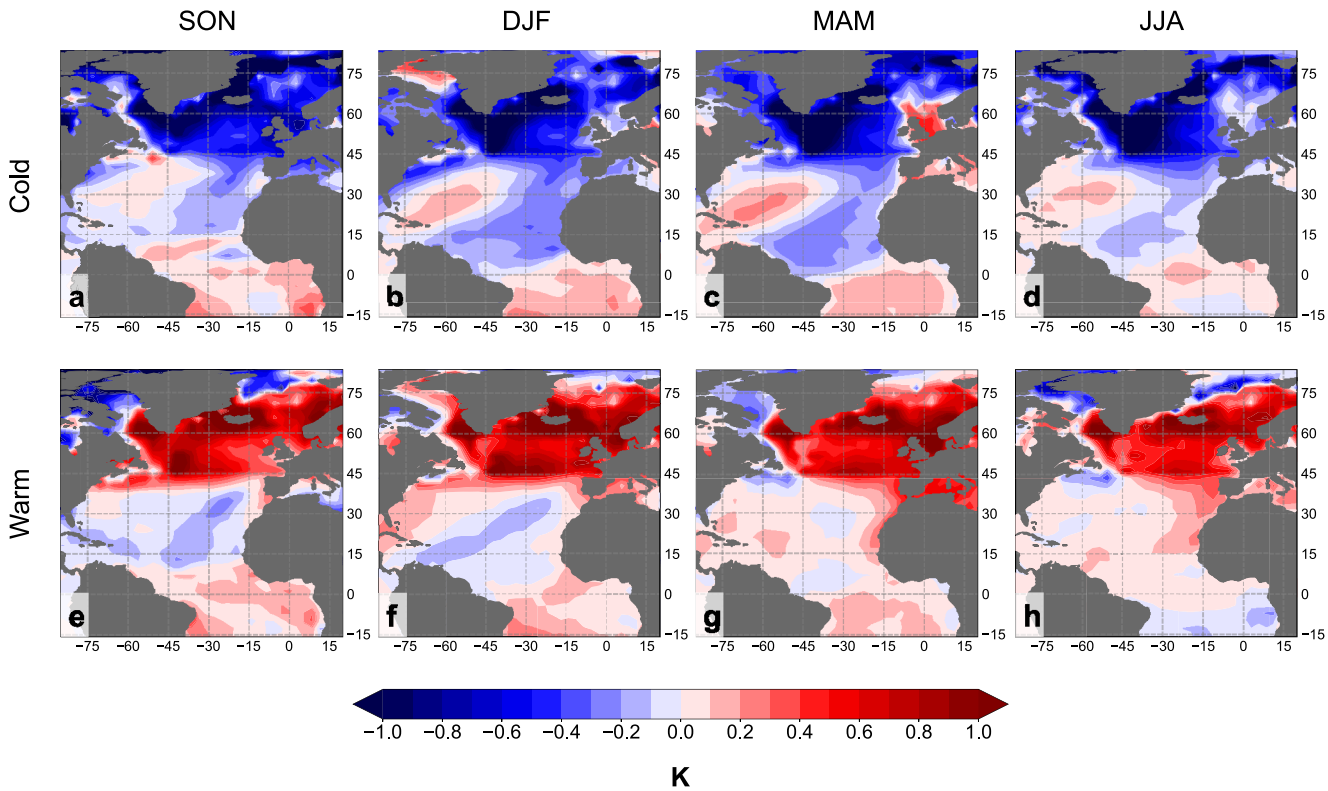

Figure 1. (a–d) Surface temperature for NEG-ML ensemble mean minus CLM-ML ensemble mean. (e and f) Same as (a–d) but for POS-ML ensemble mean minus CLM-ML ensemble mean. SON shows September-October-November means. DJF shows December-January-February means. MAM shows March-April-May means. JJA shows June-July-August means. The mixed-layer experiments have over the subpolar Atlantic (i) an imposed Q-flux term designed to maintain the AMV patterns and (ii) an interactive Q-flux component arising from the atmosphere and its interaction with the mixed-layer.

Atlantic sector, as imposed AMV anomalies may change the model mean state elsewhere through non-linearities in teleconnections.

3. Results

3.1. Atlantic-Wide SST Response

We first isolate the surface temperature response in the Atlantic sector when cold and warm anomalies are imposed in the subpolar region without ocean dynamics (Figure 1). In NEG-ML (Figures 1a–1d), cold anomalies extend immediately southward along the eastern North Atlantic subtropical basin. These anomalies strengthen throughout December-February and extend into the tropical Atlantic, such that a horseshoe pattern of surface temperature anomalies resembling the canonical cold AMV phase fully develops by the end of February. This cold AMV phase persists until ~ May, after which the pattern decays. In POS-ML (Figures 1e–1h), the imposed warm SST anomalies do not similarly spread into the tropics, notwithstanding modest warming along the eastern North Atlantic subtropical basin that occurs around May. A full canonical pattern of AMV warming spanning the North Atlantic never develops in POS-ML (see Figure S1 in the Supporting Information S1 for the last month of this experiment). The Basin-wide surface temperature response to the warm anomalies in the subpolar Atlantic thus are asymmetric, both in timing and pattern, to that of the cold anomalies. We note that such asymmetric atmospheric responses to heat anomalies have previously been shown to occur outside of a narrow range of anomalies and/or when the sign of the anomalies is reversed (Kushnir et al., 2002; Lunkeit & von Detten, 1997; Robinson et al., 2003).

To demonstrate the robustness of the above-mentioned results, we perform Empirical Orthogonal Functions (EOF) analyses on tropical Atlantic surface temperature responses to forcings across the 60-member ensemble space (Figure 2); the EOF is performed on the average of the 13-months of the experiment and without removing

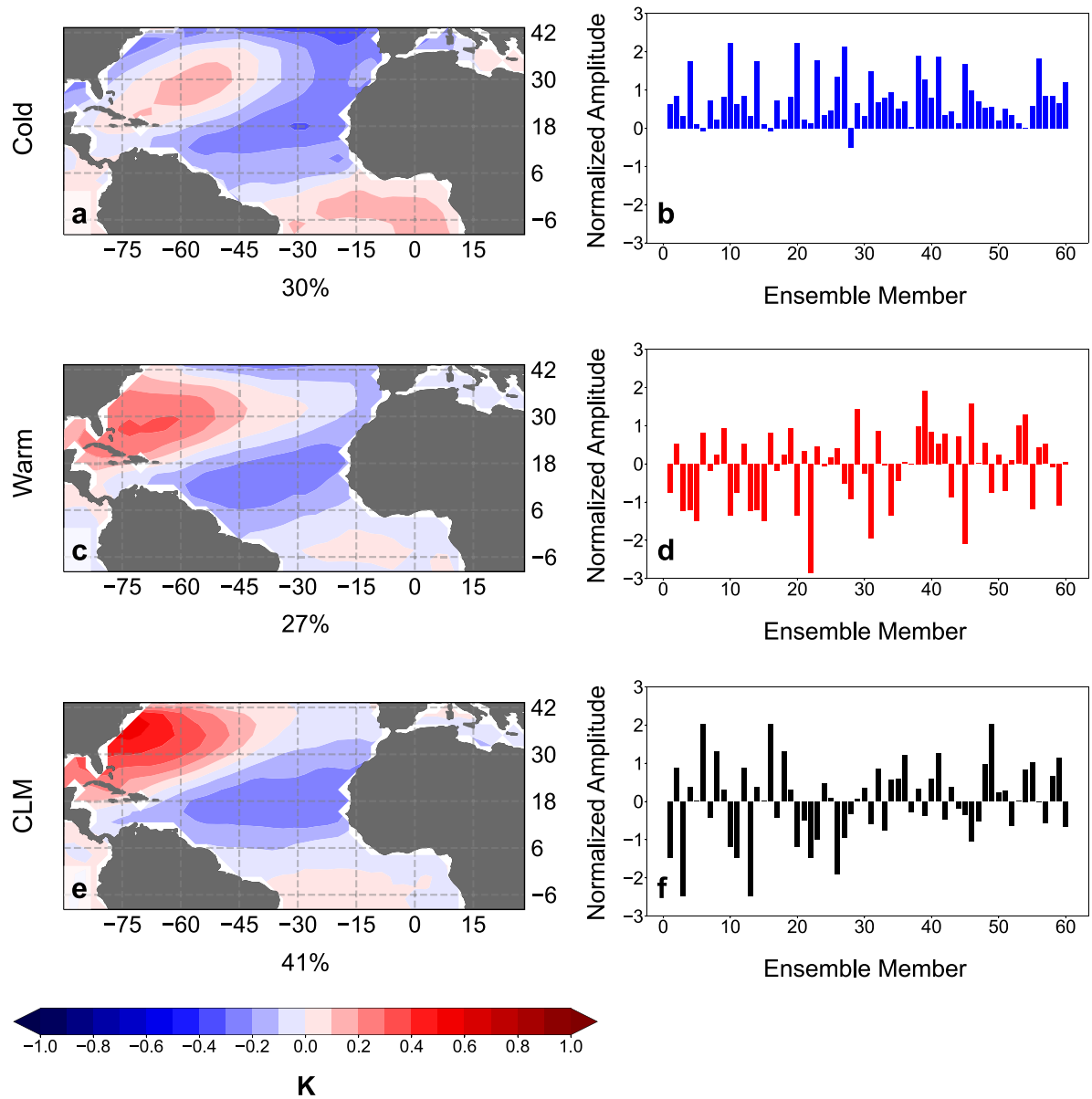

Figure 2. (left) The structure function (identified without removing the mean prior to EOF analysis) multiplied by the square root of its eigenvalue and (right) its normalized amplitude in each ensemble member corresponding to the leading principal component of the 13-month average tropical Atlantic surface temperature response in (a and b) NEG-ML members minus CLM-ML ensemble mean, (c and d) POS members minus CLM ensemble mean, and (e and f) CLM members minus CLM ensemble mean. The variance explained by each respective structure function is indicated below the corresponding panel.

the ensemble mean, in order to preserve the spatial structure common across the 60 members. Notably, the leading pattern of NEG-ML minus CLM-ML ensemble mean (Figure 2a; accounting for 30% of variance) strongly resembles the composites over the tropical Atlantic found in Figures 1a–1d, with pattern amplitudes that are steady and mostly of the same sign across the respective 60-member ensemble (Figure 2b; average normalized amplitude is 0.76 across the ensemble). The leading pattern of POS-ML minus CLM-ML ensemble mean (Figure 2c; 27% of variance), in contrast, strongly resembles that of CLM-ML minus CLM-ML ensemble mean (Figure 2e; i.e., climate "noise" due to atmospheric variability) over the Atlantic sector. The pattern amplitudes for POS-ML minus CLM-ML ensemble mean furthermore fluctuate and change signs (Figure 2d; average normalized amplitude is −0.12 across the ensemble), similar to what is seen in CLM-ML minus CLM-ML ensemble mean (Figure 2f; average normalized amplitude is 0.00 across the ensemble). Collectively, our EOF results suggest that the ensemble

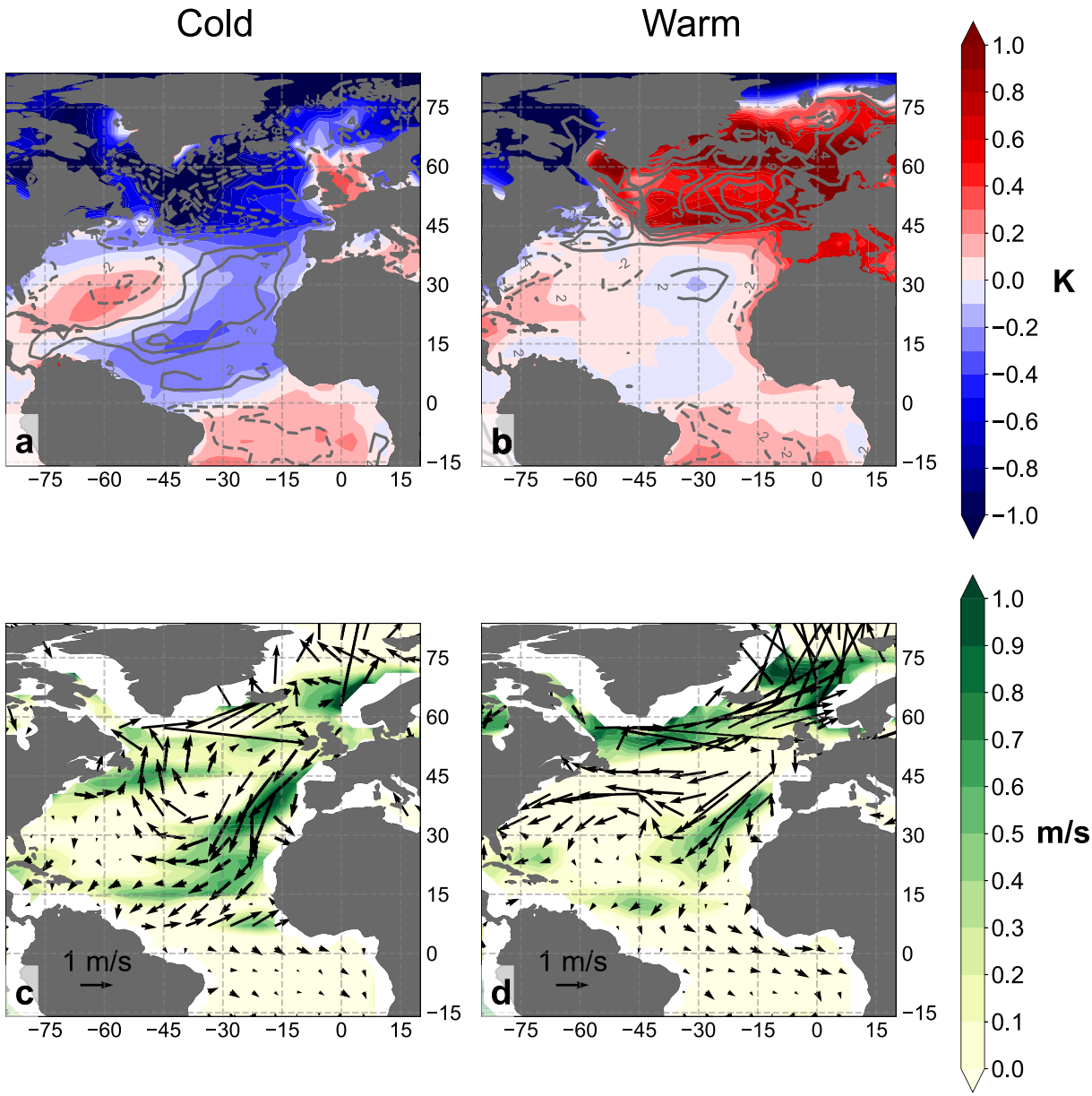

Figure 3. (top) March surface temperature field (colors) superimposed by September to February (i.e., first six months of the experiment) average latent heat flux (contours; W/m^2) for (a) NEG-ML ensemble mean minus CLM-ML ensemble mean and (b) POS-ML ensemble mean minus CLM-ML ensemble mean. Solid contours are positive values; dotted contours are negative values; zero contours are not shown. (bottom) September–October averages (i.e., first two months of the experiment) of 1,000 mbar monthly mean winds (vectors showing mean zonal and meridional winds; U and V) and wind speeds (colors; calculated on winds squared; UU and VV) for (c) NEG-ML ensemble mean minus CLM-ML ensemble mean and (d) POS-ML ensemble mean minus CLM-ML ensemble mean.

mean surface temperature response emerging in the NEG-ML, but not POS-ML, are robust and present across nearly all 60 members.

3.2. Mechanisms

We next investigate the atmospheric mechanisms by which SST anomalies propagate to the tropical Atlantic. Figure 3 shows the September–February averaged latent heat flux anomaly field, with positive values implying excess evaporation (i.e., that heat is transferred from the ocean to the atmosphere), superimposed onto the March SST field, as well as 1,000 mbar averaged wind vectors and wind speeds for September to October. For NEG-ML, the six-month cumulative effect of latent heat flux is negative (i.e., the anomalous heat flux is downward, from

the atmosphere to the ocean) over the subpolar Atlantic. This heat exchange acts to dampen the imposed SST cooling in the subpolar Atlantic (Figure 3a). In contrast, positive latent heat fluxes forces cooling along the eastern subtropical North Atlantic basin, consistent with the evolution of temperature anomalies in Figures 1a–1d. These upward latent heat flux anomalies appear to be forced in part by an anomalous circulation response to the cold subpolar SSTs that is set up immediately in the first month of the runs (Figure S2 in the Supporting Information S1). This dynamical response drives northerly, cold anomalous surface winds from the subpolar region along the eastern subtropical Atlantic (Figure 3c); from the subtropics, the SST cooling spreads into the tropics by wind-driven evaporation (wind-evaporation-SST feedback according to Xie & Philander, 1994). Sensible heat fluxes play a small role, indicating that the atmospheric bridge depends predominantly on wind-driven latent fluxes (Figure S3 in the Supporting Information S1). Note that the high-pressure circulation anomaly in the eastern subpolar gyre (Figure 3c) transports warm subtropical air northward to help balance the imposed surface cooling there. This combined dynamical (in the extratropics) and thermodynamical (in the tropics) response change appear to be set up by the initial response to the imposed SST anomaly.

As expected in the warming experiment, there is strong upward latent heat flux over the Atlantic subpolar gyre due to the excess heat imposed at the surface of the subpolar Atlantic gyre (Figure 3b). Surprisingly, the atmospheric response in POS-ML show broad similarity to that over the NEG-ML over the subpolar latitudes (i.e., anticyclonic anomalies at 1,000 mbar centered around 50°N/30°W; Figure 3d; Figure S2 in the Supporting Information S1). However, the primary interaction of the Atlantic subpolar gyre appears to be confined within the subpolar and Arctic regions with little extension to the tropical Atlantic and with intensified, strong westerly winds over the imposed positive SST anomaly. This dynamical circulation response prevents the spread of heat to the tropics, blocking the change in surface temperatures there. Consistently, the wind response over the tropical Atlantic is more subdued relative to that in the cooling experiment, although there is some wind-driven evaporative *cooling* along the eastern subtropical North Atlantic basin. Notably, neither latent heat fluxes nor winds explain the modest tropical North Atlantic warming towards the end of the POS-ML experiment (Figure S1 in the Supporting Information S1), indicating that this warming results from dynamics separate from those relevant to NEG-ML (there is a possible role for cloud cover affecting surface solar heating in POS-ML; Figure S4 in the Supporting Information S1). Collectively, in our slab-ocean experiments, the atmosphere is effective only in bridging cold SST anomalies to the tropical North Atlantic predominantly via wind-driven latent heat fluxes.

3.3. Asymmetry in Fully Coupled Model Experiments

The asymmetric response to imposed subpolar Atlantic heat anomalies persists in the CESM1 fully coupled experiments (i.e., with the addition of a dynamical ocean; Figure 4 and Figure S5 in the Supporting Information S1). Temperature anomaly patterns isolated using CLM* closely resemble those observed in the slab ocean experiments: the cooling imposed over the Atlantic subpolar gyre in the SPG_AMV− experiment spreads along the eastern subtropical North Atlantic basin to form a horseshoe pattern of cold anomalies (Figure 4a); the imposed warming in the SPG_AMV+ experiment is confined to the subpolar Atlantic gyre with little to no heating in the tropical Atlantic, similar to what is seen in POS-ML (Figure 4b). EOF analyses parallel to the ones above yield similar results and confirm the asymmetry to be robust across the 30-member ensemble (Figure 4. For instance, the leading pattern of NEG minus CLM* (Figure 4c; accounting for 29% of variance) strongly resembles that of NEG-ML minus CLM-ML ensemble mean (accounting for 30% of variance) with pattern amplitudes that are also mostly of the same sign across the ensemble (Figure 4e). The leading pattern of POS minus CLM* (Figure 4d; accounting for 26% of variance) also strongly resembles that of POS-ML minus CLM-ML ensemble mean (accounting for 27% of variance) with pattern amplitudes that fluctuate and change signs (Figure 4f). The fully coupled climate system, much like the atmosphere, thus appears to be effective in propagating only imposed cool anomalies from the subpolar Atlantic gyre to the tropical Atlantic. That is, the CESM1 fully coupled experiments confirm that the asymmetric atmospheric-mixed layer response is not limited to the idealized setting of the slab-ocean experiments. Rather, the asymmetric response is simulated even when the dynamics of the fully coupled ocean model (and any biases therein) are incorporated.

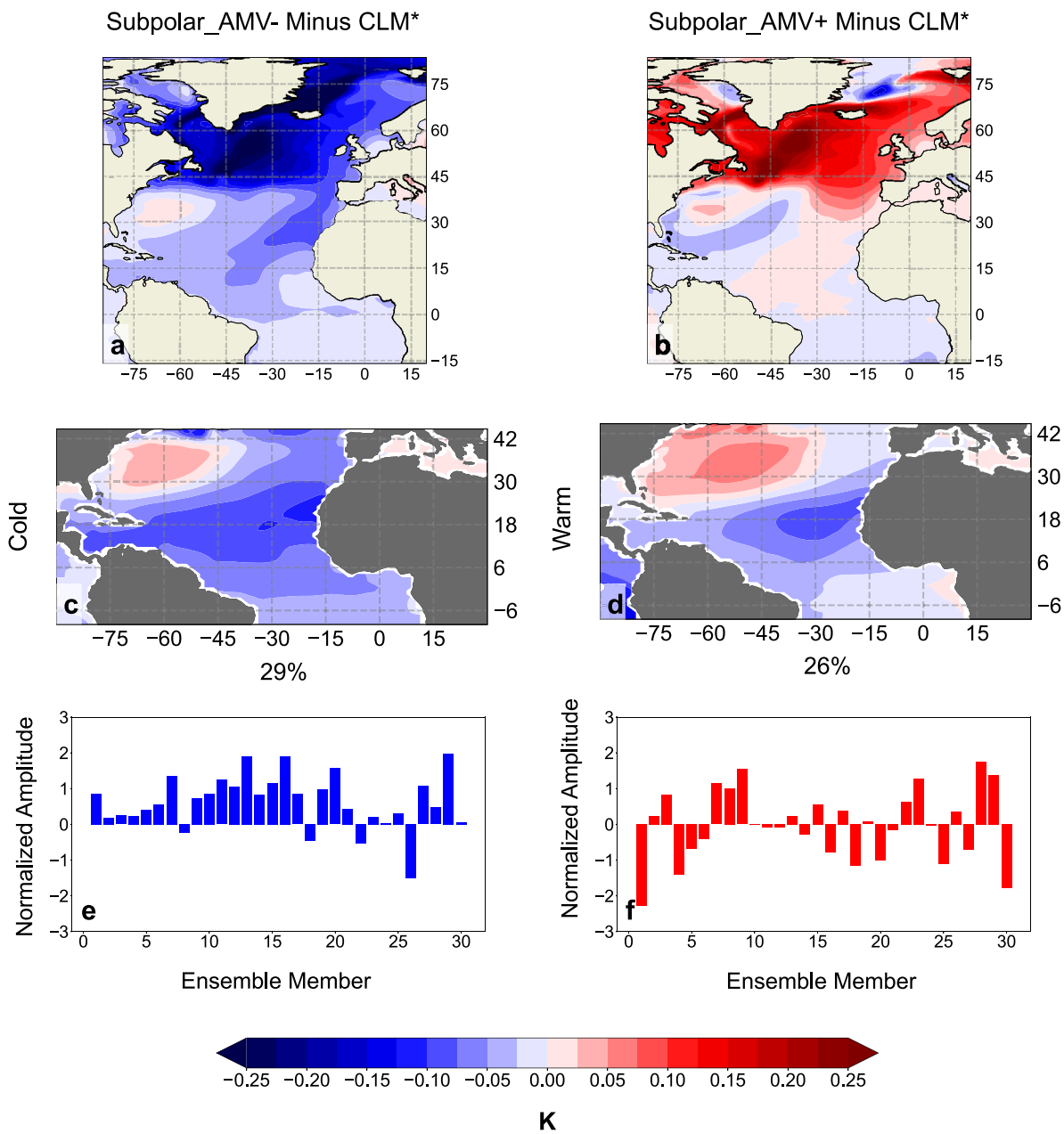

Figure 4. (top) Average surface temperature difference for (a) SPG_AMV− ensemble mean minus CLM* ensemble mean and (b) SPG_AMV+ ensemble mean minus CLM* ensemble mean for the 10 years of the CESM1 experiments. (middle) The structure function (identified without removing the mean prior to empirical orthogonal functions analysis) multiplied by the square root of its eigenvalue and (bottom) its normalized amplitude in each ensemble member corresponding to the leading principal component of the 13-month average tropical Atlantic surface temperature response in (c–e) SPG_AMV− members minus CLM* and (d–f) SPG_AMV+ members minus CLM*. The variance explained by each respective structure function is indicated below the corresponding panel.

4. Conclusion

Using idealized experiments, we have characterized a robust asymmetry in the atmospheric response to plausible ocean and/or atmosphere-induced subpolar Atlantic SST change. In our cold subpolar SST experiment, a combination of (i) a dynamical circulation response in the extratropical atmosphere followed by (ii) a thermodynamic wind-evaporation-SST response in the tropics generates wind-driven evaporative cooling that communicates the cooling from the Atlantic subpolar gyre to the tropical North Atlantic. The resulting ocean surface heat loss reproduces the canonical cold AMV SST horseshoe pattern. Notably, no such atmospheric bridge is found in our warm experiment. Instead, the primary atmospheric interaction of the Atlantic subpolar gyre is confined to the

subpolar and Arctic regions, with muted wind response or spreading of heat to the tropics. The addition of a fully dynamical ocean does not eradicate the asymmetric atmospheric response: rather, similar asymmetric surface temperature responses to parallel cooling and warming of the Atlantic subpolar gyre are observed.

Though consistent across both the slab-ocean and fully coupled model experiments, our results nevertheless depend on a single model lineage from the National Center for Atmospheric Research (NCAR); the possibility for model dependency and/or model biases are therefore a caveat to our results. Furthermore, although we have demonstrated a coherent mechanism for how the asymmetry occurs, we do not herein provide a clear physical explanation for *why*. We hypothesize that the asymmetry may arise because it is thermodynamically more efficient for subpolar Atlantic cold anomalies to draw heat from the warm tropics but for subpolar Atlantic warm anomalies to release heat into the cold polar region. This is consistent with the observation that the primary interaction of winds over the Atlantic subpolar gyre is with the tropical Atlantic in the cold experiments but with the subpolar and Arctic regions in the warm experiments (with warm air flowing towards the Arctic). The caveat of model dependence and a causal explanation notwithstanding, our results highlight a key dynamical feature of AMV for which warm and cold phases are not opposite phases of the same cycle, with important implications for how the expected future release of continental ice sheet melt into the subpolar Atlantic gyre may influence the global climate.

Data Availability Statement

The CAM5 slab-ocean model experiments are available at (http://kage.ldeo.columbia.edu:81/OTHER/.kushnir/.AMV_ML/). The CESM1 fully coupled model experiments are available at (https://doi.org/10.26024/rn3t-ep30).

Acknowledgments
This work was supported by the Flint Fellowship of Yale University, NSF AGS-1560844, and National Oceanic and Atmospheric Administration (NOAA). NA20OAR4310379. D. E. Lee was supported by National Research Foundation of Korea (NRF-2019R1A2C1090009).

References

Bellomo, K., Murphy, L. N., Cane, M. A., Clement, A. C., & Polvani, L. M. (2018). Historical forcings as main drivers of the Atlantic multidecadal variability in the CESM large ensemble. *Climate Dynamics*, *50*(910), 3687–3698. https://doi.org/10.1007/s00382-017-3834-3

Booth, B. B. B., Dunstone, N. J., Halloran, P. R., Andrews, T., & Bellouin, N. (2012). Aerosols implicated as a prime driver of twentieth-century North Atlantic climate variability. *Nature*, *484*(7393), 228–232. https://doi.org/10.1038/nature10946

Brown, P. T., Lozier, M. S., Zhang, R., & Li, W. (2016). The necessity of cloud feedback for a basin-scale Atlantic Multidecadal Oscillation, *Geophysical Research Letters*, *43*, 3955–3963. https://doi.org/10.1002/2016GL068303

Buckley, M. W., Ponte, R. M., Forget, G., & Heimbach, P. (2014). Low-frequency SST and upper-ocean heat content variability in the North Atlantic. *Journal of Climate 27*(13), 4996–5018. https://doi.org/10.1175/JCLI-D-13-00316.1>

Buckley, M. W., & Marshall, J. (2016). Observations, inferences, and mechanisms of the Atlantic Meridional Overturning Circulation: A review. *Reviews of Geophysics*, *54*(1), 5–63. https://doi.org/10.1002/2015RG000493

Buckley, M. W., Ponte, R. M., Forget, G., & Heimbach, P. (2015). Determining the origins of advective heat transport convergence variability in the North Atlantic. *Journal of Climate*, *28*(10), 3943–3956. https://doi.org/10.1175/JCLI-D-14-00579.1

Castruccio, F. S., Ruprich-Robert, Y., Yeager, S. G., Danabasoglu, G., Msadek, R., & Delworth, T. L. (2019). Modulation of Arctic sea ice loss by atmospheric teleconnections from Atlantic multidecadal variability. *Journal of Climate*, *32*(5), 1419–1441. https://doi.org/10.1175/JCLI-D-18-0307.1

Chiang, J. C. H., Cheng, W., & Bitz, C. M. (2008). Fast teleconnections to the tropical Atlantic sector from Atlantic thermohaline adjustment. *Geophysical Research Letters*, *357*, L07704. https://doi.org/10.1029/2008GL033292

Clement, A., Bellomo, K., Murphy, L. N., Cane, M. A., Mauritsen, T., Rädel, G., & Stevens, B. (2015). The Atlantic Multidecadal Oscillation without a role for ocean circulation. *Science*, *350*(6258), 320–324. https://doi.org/10.1126/science.aab3980

Delworth, T. L., & Mann, M. E. (2000). Observed and simulated multidecadal variability in the Northern Hemisphere. *Climate Dynamics*, *16*(9), 661–676. https://doi.org/10.1007/s003820000075

Enfield, D. B., Mestas-Nuñez, A. M., & Trimble, P. J. (2001). The Atlantic Multidecadal Oscillation and its relation to rainfall and river flows in the continental U.S. *Geophysical Research Letters*, *28*(10), 2077–2080. https://doi.org/10.1029/2000GL012745

Folland, C., Palmer, T., & Parker, D. (1986). Sahel rainfall and worldwide sea temperatures, 1901–85. *Nature*, *320*, 602–607. https://doi.org/10.1038/320602a0

Hastenrath, S., & Greischar, L. (1993). Circulation mechanisms related to northeast Brazil rainfall anomalies. *Journal of Geophysical Research*, *98*(D3), 5093–5102. https://doi.org/10.1029/92JD02646

Hu, Q., Feng, S., & Oglesby, R. J. (2011). Variations in North American summer precipitation driven by the Atlantic multidecadal oscillation. *Journal of Climate*, *24*, 5555–5570. https://doi.org/10.1175/2011JCLI4060.1

Hunke, E. C. & Lipscomb, W. H. (2008). CICE: The Los Alamos Sea Ice Model. Documentation and software user's manual. Version 4.0. T-3 fluid dynamics group, Los Alamos National Laboratory, Technical Report LA-CC-06–012.

Hurrell, J. W., Holland, M. M., Gent, P. R., Ghan, S., Kay, J. E., Kushner, P. J., et al. (2013). The community earth system model: A framework for collaborative research. *Bulletin of the American Meteorological Society*, *94*(9), 1339–1360. https://doi.org/10.1175/BAMS-D-12-00121.1

Knight, J. R., Allan, R. J., Folland, C. K., Vellinga, M., & Mann, M. E. (2005). A signature of persistent natural thermohaline circulation cycles in observed climate. *Geophysical Research Letters*, *32*(20), L20708. https://doi.org/10.1029/2005GL024233

Knight, J. R., Folland, C. K., & Scaife, A. A. (2006). Climate impacts of the Atlantic Multidecadal Oscillation. *Geophysical Research Letters*, *33*(17). https://doi.org/10.1029/2006GL026242

Kushnir, Y. (1994). Interdecadal variations in North Atlantic sea surface temperature and associated atmospheric conditions. *Journal of Climate*. *7*(1), 141–157. https://doi.org/10.1175/1520-0442(1994)007<0141:IVINAS>2.0.CO;2

Kushnir, Y., Robinson, W. A., Bladé, I., Hall, N. M. J., Peng, S., & Sutton, R. (2002). Atmospheric GCM response to extratropical SST anomalies: Synthesis and evaluation. *Journal of Climate*, *15*(16), 2233–2256. https://doi.org/10.1175/1520-0442(2002)015<2233:AGRTES>2.0.CO;2

Kushnir, Y., Seager, R., Ting, M., Naik, N., & Nakamura, J. (2010). Mechanisms of tropical Atlantic SST influence on North American precipitation variability. *Journal of Climate*, *23*(21), 5610–5628. https://doi.org/10.1175/2010JCLI3172.1

Kushnir, Y., & Stein, M. (2010). North Atlantic influence on 19th–20th century rainfall in the Dead Sea watershed, teleconnections with the Sahel, and implication for Holocene climate fluctuations. *Quaternary Science Reviews*, *29*, 3843–3860. https://doi.org/10.1016/j.quascirev.2010.09.004

Lee, D. E., Ting, M., Vigaud, N., Kushnir, Y., & Barnston, A. G. (2018). Atlantic Multidecadal Variability as a modulator of precipitation variability in the southwest United States. *Journal of Climate*, *31*(14), 5525–5542. https://doi.org/10.1175/JCLI-D-17-0372.1

Lozier, M. (2010). Deconstructing the conveyor belt. *Science*, *328*, 1507–1511. https://doi.org/10.1126/science.1189250

Lunkeit, F., & von Detten, Y. (1997). The linearity of the atmospheric response to North Atlantic sea surface temperature anomalies. *Journal of Climate*, *10*(12), 3003–3014. https://doi.org/10.1175/1520-0442(1997)010<3003:TLOTAR>2.0.CO;2

Martin, E. R., Thorncroft, C., & Booth, B. B. B. (2014). The multidecadal Atlantic SST—Sahel rainfall teleconnection in CMIP5 simulations. *Journal of Climate*, *27*(2), 784–806. https://doi.org/10.1175/JCLI-D-13-00242.1

Murphy, L. N., Bellomo, K., Cane, M., & Clement, A. (2017). The role of historical forcings in simulating the observed Atlantic Multidecadal Oscillation. *Geophysical Research Letters*, *44*(5), 2472–2480. https://doi.org/10.1002/2016GL071337

Naidu, P. D., Ganeshram, R., Bollasina, M. A., et al (2020). Coherent response of the Indian Monsoon Rainfall to Atlantic Multi-Decadal Variability over the last 2000 years. *Science Reports*, *10*, 1302. https://doi.org/10.1038/s41598-020-58265-3

Oelsmann, J., Borchert, L., Hand, R., Baehr, J., & Jungclaus, J. H. (2020). Linking ocean forcing and atmospheric interactions to Atlantic multidecadal variability in MPI-ESM1.2. *Geophysical Research Letters*, *47*, e2020GL087259. https://doi.org/10.1029/2020GL087259

Otterå, O. H., Bentsen, M., Drange, H., & Suo, L. (2010). External forcing as a metronome for Atlantic multidecadal variability. *Nature Geoscience*, *3*(10), 688–694. https://doi.org/10.1038/ngeo955

Robinson, W. A., Li, S., & Peng, S. (2003). Dynamical nonlinearity in the atmospheric response to Atlantic sea surface temperature anomalies. *Geophysical Research Letters*, *30*(20). https://doi.org/10.1029/2003GL018416

Ruprich-Robert, Y., Msadek, R., Castruccio, F., Yeager, S., Delworth, T., & Danabasoglu, G. (2017). Assessing the climate impacts of the observed Atlantic multidecadal variability using the GFDL CM2.1 and NCAR CESM1 global coupled models. *Journal of Climate*, *30*(8), 2785–2810. https://doi.org/10.1175/JCLI-D-16-0127.1

Schlesinger, M., & Ramankutty, N. (1994). An oscillation in the global climate system of period 65–70 years. *Nature*, *367*, 723–726. https://doi.org/10.1038/367723a0

Sutton, R. T., & Hodson, D. L. R. (2007). Climate response to basin-scale warming and cooling of the North Atlantic Ocean. *Journal of Climate*, *20*, 891–907. https://doi.org/10.1175/JCLI4038.1

Sutton, R. T., McCarthy, G. D., Robson, J., Sinha, B., Archibald, A. T., & Gray, L. J. (2018). Atlantic Multidecadal Variability and the U.K. ACSIS program. *Bulletin of the American Meteorological Society*, *99*(2), 415–425. https://doi.org/10.1175/BAMS-D-16-0266.1

Terray, L. (2012). Evidence for multiple drivers of North Atlantic multi-decadal climate variability. *Geophysical Research Letters*, *39*, L19712. https://doi.org/10.1029/2012GL053046

Ting, M., Kushnir, Y., Seager, R., & Li, C. (2009). Forced and internal twentieth-century SST trends in the North Atlantic. *Journal of Climate*, *22*(6), 1469–1481. https://doi.org/10.1175/2008JCLI2561.1

Xie, S. P., & Philander, S. G. H. (1994). A coupled ocean-atmosphere model of relevance to the ITCZ in the eastern Pacific. *Tellus A: Dynamic Meteorology and Oceanography*, *46*(4), 340–350. https://doi.org/10.3402/tellusa.v46i4.15484

Yuan, T., Oreopoulos, L., Zelinka, M., Yu, H., Norris, J. R., Chin, M., et al. (2016). Positive low cloud and dust feedbacks amplify tropical North Atlantic Multidecadal Oscillation. *Geophysical Research Letters*, *43*(3), 1349–1356. https://doi.org/10.1002/2016GL067679

Zampieri, M., Toreti, A., Schindler, A., Scoccimarro, E., & Gualdi, S. (2017). Atlantic multi-decadal oscillation influence on weather regimes over Europe and the Mediterranean in spring and summer. *Global and Planetary Change*, *151*, 92–100. https://doi.org/10.1016/j.gloplacha.2016.08.014

Zhang, R., & Delworth, T. L. (2006). Impact of Atlantic Multidecadal Oscillations on India/Sahel rainfall and Atlantic hurricanes. *Geophysical Research Letters*, *33*, L17712. https://doi.org/10.1029/2006GL026267

Zhang, R., Delworth, T. L., Sutton, R., Hodson, D. L. R., Dixon, K. W., Held, I. M., et al (2013). Have aerosols caused the observed Atlantic multidecadal variability? *Journal of the Atmospheric Sciences*, *70*(4), 1135–1144. https://doi.org/10.1175/Jas-D-12-0331.1

Zhang, R., Sutton, R., Danabasoglu, G., Kwon, Y.-O., Marsh, R., Yeager, S. G., et al (2019). A review of the role of the Atlantic meridional overturning circulation in Atlantic multidecadal variability and associated climate impacts. *Reviews of Geophysics*, *57*(2), 316–375. https://doi.org/10.1029/2019RG000644